

# Research on dynamic balancing simulation of rotary shaft based on ADAMS

Weiqliang Zheng<sup>1</sup>, Chengjie Rui<sup>1</sup>, Jie Yang<sup>1</sup> and Pingyi Liu<sup>1</sup>

<sup>1</sup>College of Engineering, China Agricultural University, Beijing 100083, China

E-mail: liupingyi@cau.edu.cn

**Abstract.** Due to the design and processing technology of rotary shaft, the mass center of it does not coincide with the rotating axis of the rotary shaft and there is an unbalanced mass. The unbalanced mass can have some disadvantages, such as the centrifugal force, the vibration and so on. Those disadvantages could reduce the accuracy and service life of the equipment. In this paper, the dynamic balance of the rotary shaft is analysed by the theory analysis combined with the dynamic simulation software. This method ensures that the rotary shaft meets the dynamic balancing requirements during the design stage. It effectively supports the structural design of the rotary shaft, and provides a way of thinking and method for the design and development of the same type of products.

## 1. Introduction

When using dynamic balancing machine to correct the unbalance of rotary components, it is necessary to install a load cell between the rotor and supporting bearing to measure the bearing force during the rotation of the rotor<sup>[1]</sup>, so as to measure the magnitude and direction of unbalance force<sup>[2-3]</sup>. It is also possible to arrange the sensor horizontally and vertically on the bearing housing supporting the rotor. First, the vibration value of the original unbalance at the measuring point is measured, and then the rotor is weighted and the vibration displacement of the bearing housing after the test weighting measured. The imbalance is corrected by calculating the influence coefficient<sup>[1,4-5]</sup>.

In this paper, theoretical analysis combined with dynamic simulation software is used in the product design of the dynamic balance of crankshaft virtual test. It provides a solution to the problem of balancing the parts where it is difficult to find an unbalanced position.

## 2. Theories and methods of dynamic balancing

When the rotor rotates, the centrifugal inertia force exists because the part has the eccentric mass, and the eccentric mass is not on the axis of rotation. That is means that the mass diameter product is not zero. Since balancing is generally carried out on both sides of the balance, the balance mass can be decomposed into two sections offset from the center of mass and perpendicular to the axis of rotation, and the imbalance mass is then balanced in both sections<sup>[1]</sup>. As shown in Figure 1:



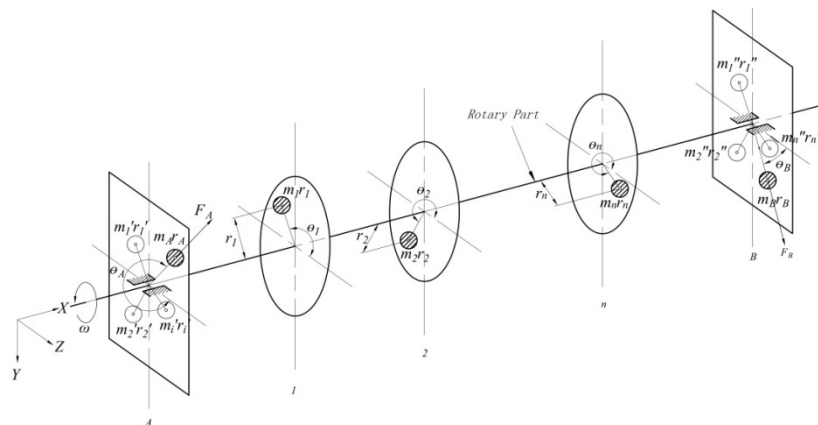


**Figure 1.** Dynamic balance principle

Because this method only obtains the unbalance and the phase by the measuring force, it only needs to balance the unbalanced amount obtained in the corresponding phase pair. It is not necessary to give the magnitude and phase of the unbalanced mass of each section, which is suitable for the motion of the irregularly shaped rotating part. Balance design issues. The position of the rotation pair is the balance cross section, and the measurement of the maximum force along the Y direction and its phase can be processed by means of virtual simulation analysis. A description will be given with examples.

### 3. Experimental Design of Crankshaft Dynamic Balancing

In this paper, the ADAMS software is used to monitor the centrifugal force and phase angle of a crankshaft. In ADAMS, imbalance balanced simulation tests are carried out to balance the existing imbalances.

#### 3.1. Model establishment

The established three-dimensional model is saved as .x\_t format, imported into ADAMS. The crankshaft material is No.45 steel, and the density is  $7850\text{kg} / \text{m}^3$ . And the mass  $m = 6.5098\text{kg}$ . The gravity is along the Y-axis positive direction in ADAMS.

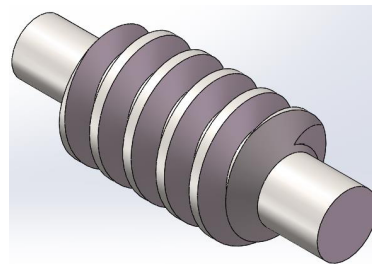


**Figure 2.** Crankshaft 3D model

#### 3.2. Dynamic balance simulation analysis

Two sections are selected for dynamic balancing. The distance from section 1 to plane A is 56.5 mm, the distance from section 2 to plane A is 69.5 mm, and rotary pair 1 and rotary pair 2 are respectively added in section 1 and section 2. Drive 1 is added in the position of the drive 1, the size of its speed is  $157\text{rad} / \text{s}$ , the direction from section 2 to section 1 as clockwise.

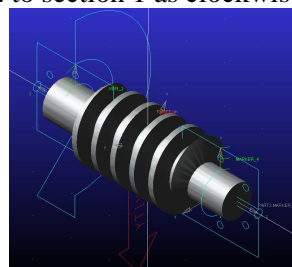


### Figure 3. Simulation analysis

Establish two measurements: measuring the magnitude of the force  $F_{Y1}$  in the positive direction of the Y-axis at the rotation pair 1, and measuring the magnitude of the force  $F_{Y2}$  that it receives in the positive direction of the Y-axis at the rotation pair 2. The simulation time is set to 0.08s (2 cycles) and the step size is set to 4000. After setting up, we carry on the simulation analysis. It can be seen that the crankshaft rotates about the X axis and the two measurements of forces  $F_{Y1}$  and  $F_{Y2}$  change periodically. The change rules are shown in Figure 4 and Figure 5.

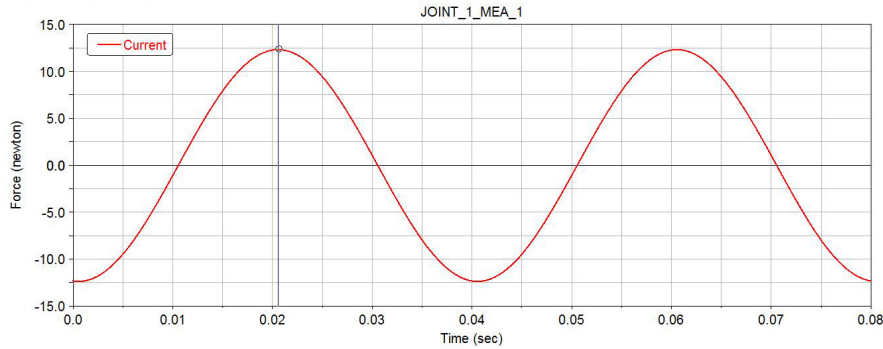


Figure 4. Curve of the force  $F_{Y1}$

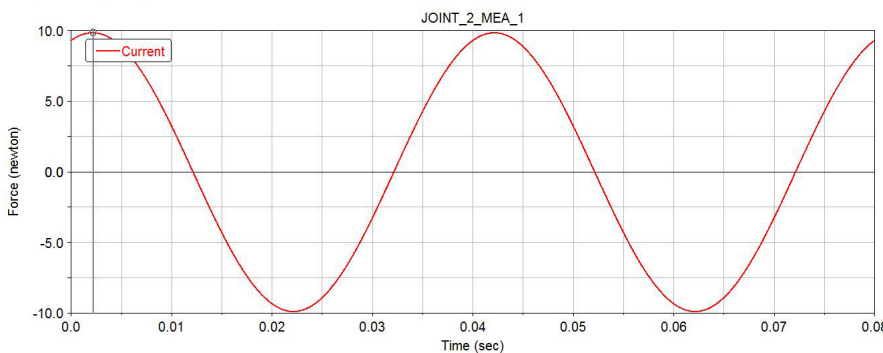


Figure 5. Curve of the force  $F_{Y2}$

Through the analysis of the curve, the maximum force  $\max(F_{Y1}) = 12.3505\text{N}$  in section 1, the phase angle is  $185.625^\circ$ ; the maximum force in section 2  $\max(F_{Y2}) = 9.8763\text{N}$ , the phase angle is  $19.665^\circ$ . Set the magnitude of the unbalance in section 1 to  $m_1r_1$  and the magnitude of the unbalance in section 2 to  $m_2r_2$ .

In section 1, the magnitude of residual unbalance  $m_1r_1$  is:

$$m_A r_A = \frac{\max(F_{Y1})}{\omega^2} = \frac{12.3505}{157^2} \times 1000 \text{g} \cdot \text{mm} = 0.5011 \text{g} \cdot \text{mm} \quad (1)$$

The phase angle  $\varphi = \theta_A = 360^\circ - 185.625^\circ = 174.375^\circ$ ;

In section 2, the magnitude of residual unbalance  $m_2r_2$  is:

$$m_B r_B = \frac{\max(F_{Y2})}{\omega^2} = \frac{9.8763}{157^2} \times 1000 \text{g} \cdot \text{mm} = 0.4007 \text{g} \cdot \text{mm} \quad (2)$$

The phase angle  $\varphi = \theta_A = 360^\circ - 19.665^\circ = 340.335^\circ$ ;

The overall balance accuracy A is calculated as follows:

$$A = \frac{m_A r_A + m_B r_B}{m} \omega = \frac{0.5011 + 0.4007}{6.5098 \times 1000} \times 157 \text{mm} / \text{s} = 0.02176 \text{mm} / \text{s} \quad (3)$$

### 3.3. Balance method of unbalance amount

First, balance the amount of unbalance in section 1. In the direction of the end plate (clockwise), remove 8.56 mm depth material in this direction at a distance of  $180^\circ + 5.625^\circ = 185.625^\circ$  from the end plate. The distance from the position where the material is removed to the origin is  $X = 53 \text{mm}$ . In

this case, the maximum force  $\max(F_{Y1}) = 0.0854\text{N}$  in section 1 and the maximum force  $\max(F_{Y2}) = 9.7915\text{N}$  in section 2, both of which have been reduced. The phase angle  $\theta_2 = 0.002185 * 9000^\circ = 19.665^\circ$  remains unchanged.

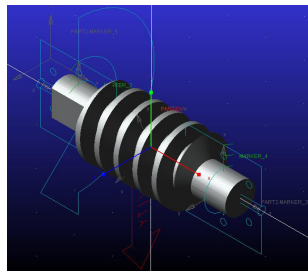


**Figure 6.** The unbalance in section 1

Then, the amount of unbalance in section 2 is balanced, and the position of mass removal is shown in FIG. 7. Seen from the end plate direction (clockwise), 5.54 mm deep material is removed in this direction at  $19.665^\circ$  from the end plateau. The distance from the side where the material is removed to the origin is  $X = 64\text{ mm}$ . In this case, the maximum force in section 2  $\max(F_{Y2}) = 0.0274\text{N}$ , and the maximum unbalance force  $\max(F_{Y1}) = 0.0907\text{N}$  in section 1, which is improved but not increased slightly.

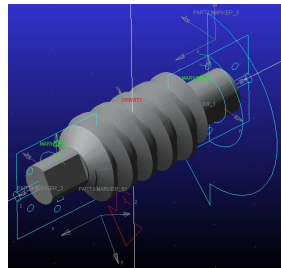


**Figure 7.** The unbalance in section 2

After the balance, the curve of internal force of the two sections is shown in Figure 8 and Figure 9:

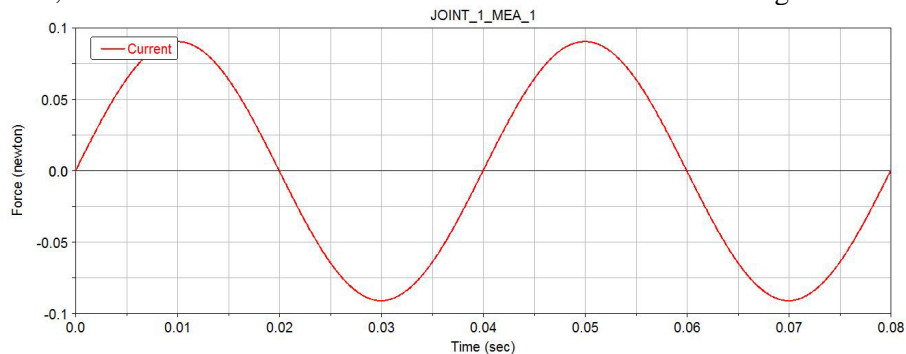


**Figure 8.** The curve of internal force of section 1

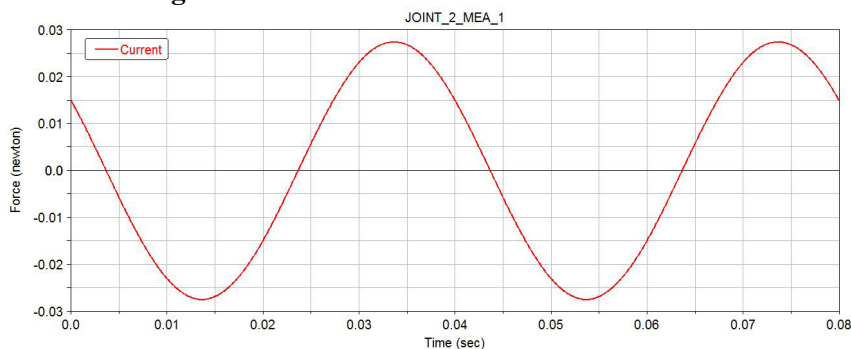


**Figure 9.** The curve of internal force of section 2

After dynamic balancing, the size of residual unbalance  $m_1r_1$  in section 1 is:

$$m_A r_A = \frac{\max(F_{Y1})}{\omega^2} = \frac{0.0907}{157^2} \times 1000 g \cdot mm = 0.00368 g \cdot mm \quad (4)$$

The phase angle  $\varphi = \theta_A = 360^\circ - 185.625^\circ = 174.375^\circ$ ;

In section 2, the size of the residual unbalance  $m_2 r_2$  is:

$$m_B r_B = \frac{\max(F_{Y2})}{\omega^2} = \frac{0.0274}{157^2} \times 1000 g \cdot mm = 0.00111 g \cdot mm \quad (5)$$

The phase angle  $\varphi = \theta_A = 360^\circ - 19.665^\circ = 340.335^\circ$ ;

The overall balance accuracy A is calculated as follows:

$$A = \frac{m_A r_A + m_B r_B}{m} \omega = \frac{0.5011 + 0.4007}{6.5098 \times 1000} \times 157 mm / s = 0.02176 mm / s \quad (6)$$

After the balance is completed, the three-dimensional solid model of the crankshaft is shown in Figure 10:

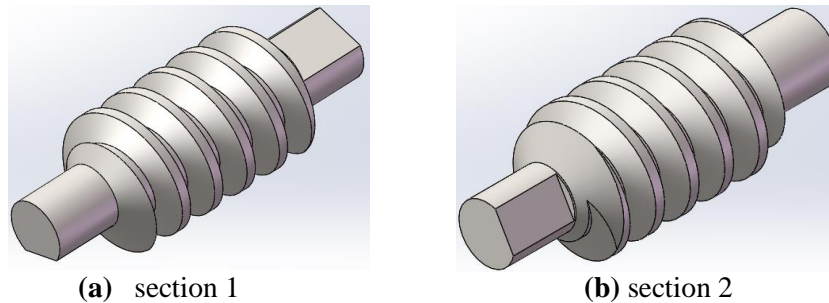


**Figure 10.** After being balanced three-dimensional solid model

#### 4. Conclusion

(1) In this paper, theoretical analysis combined with dynamic simulation software is used in the product design of the dynamic balance of crankshaft virtual test, effectively support the structure of the crankshaft design, and provides a design method for the same type of product.

(2) After the crankshaft is dynamically balanced by this method, the magnitude of the residual unbalance in section 1 is 0.00368 g · mm, the residual unbalance in section 2 is 0.00111 g · mm, and the overall balance accuracy is 0.02176 mm / s, the result meets the design requirements.

#### 5. References

- [1] Zhou S. Modeling Estimation and Active Balancing of Speed Varying Rotor System. Ann Arbor: University of Michigan. 2001:15~16
- [2] A Gusarov VIS, U I Susanin Automatic Balancing of Rotors by the Application of Servo Systems Moscow: Izdatel'stvo Nauka, 1974.177-172
- [3] C.H.Chen,K.W.Wang. An Integrated Approach Toward the Dynamic Analysis of High-Speed Spindles[J].Vibration and Acoustics,1994,116:514-522.
- [4] Kim S M, ee S K, ee K J. Effect of Bearing Surroundings on the High-Speed Spindle-Bearing Compliance[J]. International Journal of Advanced Manufacturing Technology, 002, 9: 551-557.
- [5] Shin Y C. Bearing Non-linearity and Stability Analysis in High Speed Machining[J]. Journal of Engineering for Industry, 992, 14: 23-30.

#### Acknowledgments

The work in this paper was fully supported by National Natural Science Foundation of China under Grant No. 51475460.